Effects of Mutagenesis of Gln97 in the Switch II Region of *Escherichia coli* Elongation Factor Tu on Its Interaction with Guanine Nucleotides, Elongation Factor Ts, and Aminoacyl-tRNA†

Tomas Navratil and Linda L. Spremulli*

Department of Chemistry, Campus Box 3290, University of North Carolina, Chapel Hill, North Carolina 27599-3290

Received May 21, 2003; Revised Manuscript Received August 25, 2003

ABSTRACT: Elongation factor Tu (EF-Tu) delivers aminoacyl-tRNA to the A-site of the ribosome. In a multiple-sequence alignment of prokaryotic EF-Tu's, Gln97 is nearly 100% conserved. In contrast, in mammalian mitochondrial EF-Tu's, the corresponding position is occupied by a conserved proline residue. Gln97 is located in the switch II region in the GDP/GTP binding domain of EF-Tu. This domain undergoes a significant structural rearrangement upon GDP/GTP exchange. To investigate the role of Gln97 in bacterial EF-Tu, the *E. coli* EF-Tu variant Q97P was prepared. The Q97P variant displayed no activity in the incorporation of [^{14}C]Phe on poly(U)-programmed *E. coli* ribosomes. The Q97P variant bound GDP more tightly than the wild-type EF-Tu with K_d values of 7.5 and 12 nM, respectively. The intrinsic rate of GDP exchange was 2−3-fold lower for the Q97P variant than for wild-type EF-Tu in the absence of elongation factor Ts (EF-Ts). Addition of EF-Ts equalized the GDP exchange rate between the variant and wild-type EF-Tu. The variant bound GTP at 3-fold lower levels than the wild-type EF-Tu. Strikingly, the Q97P variant was completely inactive in ternary complex formation, accounting for its inability to function in polymerization. The structural basis of these observations is discussed.

Elongation factor Tu (EF-Tu[1]) plays an essential role in the elongation phase of protein synthesis. EF-Tu·GTP binds aminoacyl-tRNA (aa-tRNA) and delivers it to the A-site of the ribosome (*1*). Upon establishment of the cognate codon−anticodon interaction, the GTPase activity of EF-Tu is triggered by the 50S subunit of the ribosome. This step is followed by rapid GTP hydrolysis, and the release of inorganic phosphate. The subsequent conformational change in EF-Tu decreases its affinity for the aa-tRNA significantly. The 3′ CCA-aa end and the acceptor stem of the aa-tRNA are released and transferred to the A-site on the 50S subunit, and EF-Tu·GDP dissociates from the ribosome. EF-Tu·GDP is recycled into its activated GTP form by the nucleotide exchange factor elongation factor Ts (EF-Ts), which accelerates the release of GDP from EF-Tu approximately 10^4-fold. EF-Tu·GTP then readily binds aa-tRNA and is prepared for another round of elongation.

Extensive crystallographic work has provided the structures of the EF-Tu·GDP complexes from *E. coli* (*2*−*4*), *Thermus aquaticus* (*5*), and bovine mitochondria (*6*). Two structures for EF-Tu·GTP are known from *Thermus thermophilus* (*7*) and *T. aquaticus* (*8*). The structures of two EF-Tu·Ts complexes from *E. coli* (*9*) and *T. thermophilus* (*10*) have been solved, and the structures of two ternary complexes of *T. aquaticus* EF-Tu·GTP with yeast Phe-tRNA^{Phe} (*11*) and *E. coli* Cys-tRNA^{Cys} (*12*) are known. For the purposes of this work, the structures of *E. coli* EF-Tu·GDP (*4*), *T. aquaticus* EF-Tu·GDP (*5*), EF-Tu·GTP (*8*), and EF-Tu·GTP with yeast Phe-tRNA^{Phe} (*11*) have been used as a starting point. *E. coli* EF-Tu is 70.6% identical to the *T. aquaticus* EF-Tu in primary sequence. The three major primary sequence differences occur in the loop regions. The root-mean-square deviation for all Cα atoms for the *E. coli* and *T. aquaticus* EF-Tu·GDP structures is 1.39 Å.

EF-Tu is a 43 kDa globular protein folded into three domains. A flexible linker of 13 residues connects domain 1 (residues 1−198) and domain 2 (amino acids 211−293). A rigid five-residue stretch connects domains 2 and 3 (residues 299−393). Domain 1 constitutes the GDP/GTP binding domain, while all three domains participate in the creation of the aa-tRNA binding site (*1*, *13*). The binding of GDP and GTP is facilitated by one Mg^{2+} ion. EF-Tu undergoes a significant structural transition between its GDP and GTP bound states (Figure 1A,B). This transition is characterized by secondary structure changes in domain 1 and by a change in the orientation of domain 1 relative to domains 2 and 3, which act as a unit. In the GTP form, domain 1 rotates by 90° relative to domains 2 and 3 compared to its position in the GDP form of EF-Tu. Domains 2 and 3 retain the same orientation with respect to each other. The large opening between the domains is closed in the GTP form, and the cleft created among domains 1−3 forms the binding site for the aa-tRNA. The structure of EF-Tu in the EF-Tu·GTP·Phe-tRNA^{Phe} complex is similar to its structure in the EF-Tu·GTP complex.

† This work has been supported by funds provided by the National Institutes of Health (Grant GM32734).

* To whom correspondence should be addressed: Phone: (919) 966-1567. Fax: (919) 966-3675. E-mail: Linda_Spremulli@unc.edu.

[1] Abbreviations: aa-tRNA, aminoacyl-tRNA; EF-Tu, elongation factor Tu also referred to as EF1a; EF-Tu$_{mt}$, mitochondrial EF-Tu; EF-Ts, elongation factor Ts also referred to as EF1b; IPTG, isopropyl thiogalactoside.

10.1021/bi034855a CCC: $25.00
Published on Web 10/30/2003

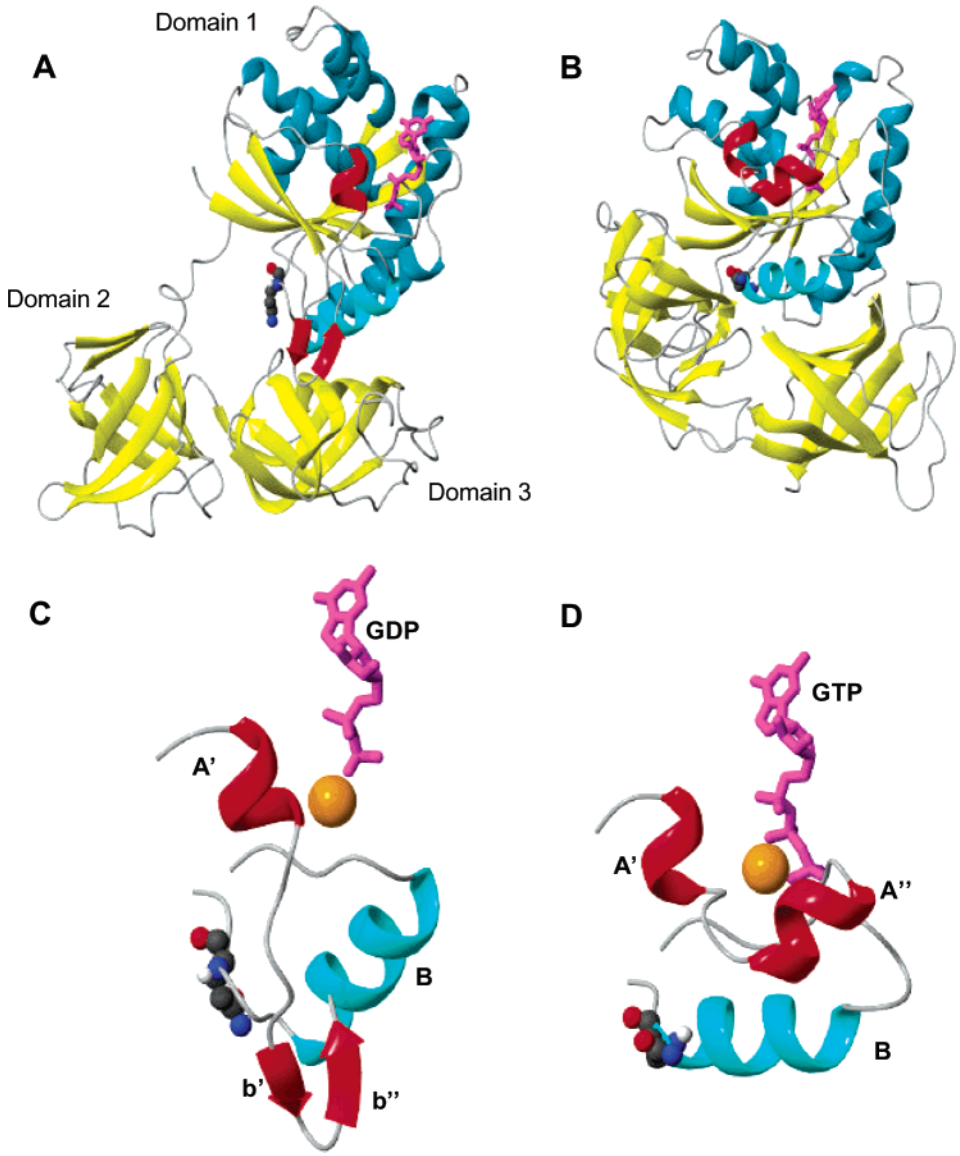

FIGURE 1: Changes in domain orientation and in switches I and II in the EF-Tu·GDP and EF-Tu·GTP complexes. (A) Crystal structure of the *T. aquaticus* EF-Tu·GDP complex (PDB 1TUI). The space-filled atoms represent the location of Gln97. (B) Crystal structure of the *T. aquaticus* EF-Tu·GTP complex (PDB 1EFT). The space-filled atoms represent the location of Gln97. (C) Crystal structure of the switch I and II regions of *T. aquaticus* EF-Tu·GDP. The space-filled atoms represent the location of Gln97. (D) Crystal structure of the switch I and II regions of *T. aquaticus* EF-Tu·GTP. The space-filled atoms represent the location of Gln97. Color coding: β-Sheets are displayed in yellow, and α-helices are displayed in aquamarine with the exception of the switch I and II regions. Switch I is displayed in red and switch II in cyan. Guanine nucleotides are in magenta. The Mg^{2+} ion is pictured in orange. The structures are displayed using MolMol (*28*) and Povray (http://www.povray.org).

The sequence of domain 1 is highly conserved in EF-Tu especially in the switch regions and the actual nucleotide binding pocket. However, one striking exception is found at position 97 (*E. coli* numbering). This residue is highly conserved as a Gln in the prokaryotic factors. However, it is a Pro in mammalian mitochondrial EF-Tu. Gln97 is involved in the structural changes in domain 1 of EF-Tu upon GDP/GTP exchange, and the side chain of Gln97 participates in the hydrogen bond network stabilizing the amino acid binding pocket of the aa-tRNA in the ternary complex (*11*, *12*). Since neither the structure of the GTP form nor the structure of the ternary complex of mitochondrial EF-Tu has been solved, it is difficult to predict how a Pro residue is accommodated in the mitochondrial factors. Hence, it was of interest to examine the effect of a Pro at this position in *E. coli* EF-Tu on the properties of the prokaryotic factor. In the current work, Gln97 was mutated to Pro and the resulting variant examined for its ability to interact with its multiple ligands.

MATERIALS AND METHODS

Materials. All materials were obtained from Sigma or Mallinckrodt. *E. coli* ribosomes were prepared as described (*14*, *15*). *E. coli* elongation factor EF-Ts was purified to homogeneity from *E. coli* as an overexpressed His-tagged protein (*16*). *E. coli* elongation factor EF-G was isolated from *E. coli* as described (*17*) and further purified by chromatography on Sephadex G-75. Information on impurities in the GDP and GTP preparations affecting their OD_{268} was obtained for each lot from Sigma quality control and used for more accurate concentration determinations by spectro-

photometry. [^{3}H]GDP and [γ-^{32}P]GTP were obtained from Dupont New England Nuclear.

Preparation and Purification of the E. coli EF-Tu Q97P Variant. The *E. coli* EF-Tu Q97P variant was prepared by a modified PCR mutagenesis protocol (*18*). The forward primer vec-2 (5′-taggggaattgtgagcggataac-3′) is complementary to a sequence of pET-24c(+) upstream of the 5′-end of the EF-Tu gene. The reverse primer vec-3 (5′-attgctcagcggtggcagcagcc-3′) is complementary to a sequence of pET-24c(+) downstream of the 3′-end of the EF-Tu gene. The forward mutagenic primer fETuQ97P (5′-ccggtgctgcgccgatggacggcgcg-3′) and the reverse mutagenic primer rETuQ97P (5′-cgcgccgtccatcggcgcagcaccgg-3′) are complementary to the Q97P region in the EF-Tu gene. A two-step PCR process generated the full EF-Tu gene including the P97Q mutation. In the first round of PCR, the complete *E. coli* EF-Tu gene in pET-24c(+) (*19*) was used as a template. PCR amplification using the forward vec-2 primer together with the reverse rETuQ97P primer and reverse vec-3 together with the forward fETuQ97P primer resulted in two EF-Tu gene fragments, both including the Q97P mutation and overlapping around the site of the mutation. The 5′-end of the EF-Tu gene fragment included an *Nde*I restriction site, while the 3′-end of the EF-Tu gene fragment included an *Xho*I restriction site. In the second round of PCR, the two overlapping fragments of the EF-Tu gene were used as templates along with the vec-2 and vec-3 primers. The product of the second round of PCR was a complete EF-Tu gene including the Q97P mutation and both *Nde*I and *Xho*I restriction sites at the corresponding 5′-end and 3′-end of the full gene. The resulting PCR product was ligated into the pET-24c(+) and transformed into *E. coli* XL-1 Blue competent cells. The clone was purified from *E. coli* XL-1 Blue and transformed into *E. coli* BL21 (DE3) for expression.

The variant and wild-type EF-Tu's were purified side-by-side under identical conditions. Cultures (100 mL) grown overnight at 37 °C in LB media (*20*) containing 25 ug/mL kanamycin were used to inoculate 2 L cultures. Cells were grown in LB containing 25 μg/mL kanamycin at 37 °C until the density reached 0.6−0.8 at A_{595}. The expression of the wild-type and variant factors was induced by the addition of 50 μM IPTG for 5 h. The wild-type and variant EF-Tu's were purified by Ni^{2+}-NTA column chromatography as described (*21*). No phosphatase activity was detected in either the wild-type or variant EF-Tu samples as assayed by a 30 min incubation with [γ-^{32}P]GTP and subsequent analysis by thin-layer chromatography. The purity of the samples was assessed by SDS−PAGE with Coomassie Blue staining. Two independent preparations of EF-Tu and the Q97P variant were tested in the assays described below. The data shown are representative of the results obtained and were completely reproducible with identical quantitative trends.

Determination of the Percentage of Active EF-Tu Molecules. Protein concentrations were determined by the Bradford assay (Biorad). It has been known for some time that not all molecules of wild-type EF-Tu are active in GDP binding (*22*). Depending on the particular sample of EF-Tu, the percentage of molecules capable of binding GDP varies from ~30% to ~80%. Therefore, the overall protein concentration as determined by Bradford assays is not an accurate measure of the concentration of EF-Tu and cannot be used for the determination of K_d values. Instead the concentration of molecules active in GDP binding was determined by a [^{3}H]GDP binding assay under saturating GDP concentrations (6.5 μM with 40 nM EF-Tu). Under these conditions 99% of the active EF-Tu molecules formed [^{3}H]GDP·EF-Tu complexes which were detected using a nitrocellulose filter binding assay (*17*). In all experiments carried out in this work the concentration of EF-Tu was determined by this method.

Removal of Excess GDP and Determination of GDP Remaining in Purified EF-Tu. In the purification of EF-Tu, 10 μM GDP is used in all buffers to preserve the activity of the protein (*21*). In addition, EF-Tu binds GDP tightly and is purified from cell extracts as an EF-Tu·GDP complex. To determine an accurate K_d for the binding of GDP to wild-type EF-Tu and its Q97P variant, the excess GDP had to be removed and the amount of GDP remaining bound to EF-Tu was determined. A sample of EF-Tu (400 μL, 600 μg of protein) was applied to a Sephadex G-50 column (13 × 180 mm) equilibrated in buffer A (42 mM Tris−HCl, pH 7.8, 8 mM $MgCl_2$, 130 mM NH_4Cl, and 4 mM dithiothreitol) at 4 °C. The column was developed with this buffer at a flow rate of 1.5 mL/min. Fractions (0.25 mL) were collected in Eppendorf tubes and immediately tested for the concentration of active EF-Tu by measuring the amount of GDP bound at saturating concentrations of GDP (6.5 μM) as described above. EF-Tu eluted from the Sephadex G-50 column as a 1:1 EF-Tu·GDP complex.

GDP Binding and EF-Ts Stimulation of GDP Exchange. GDP binding measurements were carried out using the filter binding assay described previously (*17*) in buffer containing 42 mM Tris−HCl, pH 7.8, 8 mM $MgCl_2$, 130 mM NH_4Cl, and 4 mM dithiothreitol. The samples of EF-Tu (6.9 nM) were incubated for 10 min at 37 °C in 6.45 nM (20074 cpm/pmol) and 20 nM (8240 cpm/pmol) [^{3}H]GDP. The specific activity of the [^{3}H]GDP was corrected for the GDP present in the EF-Tu samples. Incubation was carried out for 10 min at 37 °C. A time course of GDP binding indicated that equilibrium had been reached in all experiments. The value for GDP binding was corrected for the amount of label retained on the filter in the absence of EF-Tu (0.01 pmol). The K_d for the reaction EF-Tu·GDP⇆EF-Tu + GDP was determined according to the following equation:

$$K_d = \frac{[\text{EF-Tu}]_f[[^3\text{H}]\text{GDP}]_f}{[[^3\text{H}]\text{GDP}\cdot\text{EF-Tu}]}$$

where $[\text{EF-Tu}]_f = [\text{EF-Tu}]_i - [\text{EF-Tu}\cdot[^3\text{H}]\text{GDP}]$, $[[^3\text{H}]\text{GDP}]_f = [[^3\text{H}]\text{GDP}]_i - [\text{EF-Tu}\cdot[^3\text{H}]\text{GDP}]$, $[\text{EF-Tu}\cdot[^3\text{H}]\text{GDP}]$ is the amount of the EF-Tu·[^{3}H]GDP complex measured, $[\text{EF-Tu}]_i$ is the initial concentration of active EF-Tu, and $[[^3\text{H}]\text{GDP}]_i$ is the initial concentration of [[^{3}H]GDP] corrected for the amount of GDP in the EF-Tu samples.

To examine the rate of GDP exchange, reaction mixtures (120 μL) containing the wild-type and variant EF-Tu·GDP complexes (83 nM) were incubated in the presence of 200 nM [^{3}H]GDP for 3, 6, and 9 min at 0 °C under ionic conditions identical to those used above. The amount of the [^{3}H]GDP·EF-Tu complex formed at each time was determined by the filter binding assay.

To observe the effect of *E. coli* EF-Ts on the rate of GDP exchange, wild-type EF-Tu and its Q97P variant (83 nM) in

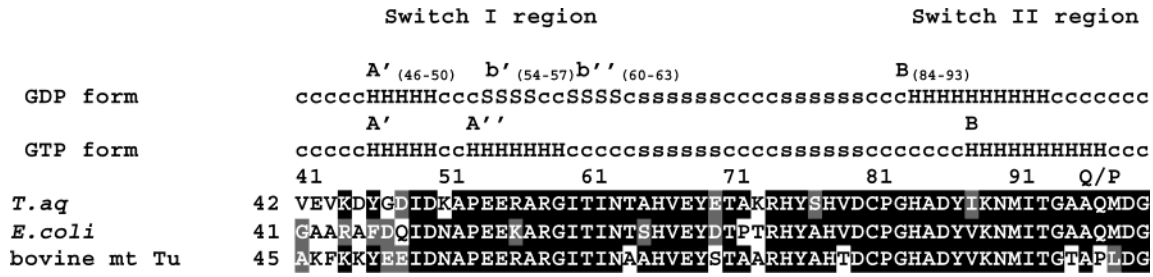

FIGURE 2: Primary sequence alignment of switches I and II of *E. coli*, *T. aquaticus*, and bovine EF-Tu$_{mt}$. The following secondary structure notation has been used: c, coil regions; S, sheet regions in switch I; s, other sheet regions; H, helical regions in switch I or II. The numbering for bovine EF-Tu$_{mt}$ is for the mature protein.

120 μL reaction mixtures were incubated with EF-Ts (8.3 nM) in the presence of 200 nM [^{3}H]GDP for 3, 6, and 9 min at 0 °C under ionic conditions identical to those of the GDP binding assay. The amount of the [^{3}H]GDP·EF-Tu complex was determined by the filter binding assay. The value for GDP exchange was corrected for the amount of label retained on the filter in the absence of EF-Tu (about 0.01 pmol) at the indicated times.

GTP Binding Measurements. The binding of [γ-^{32}P]GTP to the wild-type EF-Tu and its Q97P variant was carried out as described above except that reaction mixtures (120 μL) contained 8 μM [γ-^{32}P]GTP (1000 cpm/pmol) and wild-type or Q97P EF-Tu (41.7, 83.3, or 125 nM). In addition, 2.5 mM phosphoenol pyruvate and 0.0025 U/μL pyruvate kinase were added to the reactions. The reactions were incubated for 10 min at 37 °C. ATP (5 mM) was then added to decrease the background by displacing the [γ-^{32}P]GTP bound to pyruvate kinase. Reaction mixtures were analyzed using the filter binding assay described previously (*17*). A blank representing the amount of label retained on the filter in the absence of EF-Tu (about 0.5 pmol) has been subtracted from each value. The amounts of the wild-type EF-Tu and the Q97P variant used were normalized in relation to their GDP binding activities; i.e., equal amounts of each protein active in GDP binding were used.

Measurement of Ternary Complex Formation. Ternary complex formation measurements were carried out basically as previously described (*22*). Ternary complexes were formed in reaction mixtures (50 μL) containing wild-type or Q97P EF-Tu (80, 160, 240, or 320 nM) and 0.54 μM [^{14}C]Phe-tRNA^{Phe} (456 cpm/pmol) at 0 °C for 30 min in buffer containing 50 mM Tris−HCl, pH 7.6, 70 mM KCl, 6.5 mM $MgCl_2$, 1 mM dithiothreitol, 4 mM phosphoenol pyruvate, and 0.005 U/μL pyruvate kinase. After formation of the ternary complex, RNase A (2 ug) was added followed by a 60 s incubation at 0 °C. This reaction was quenched by the addition of cold 5% trichloroacetic acid, and the amount of [^{14}C]Phe-tRNA^{Phe} remaining was determined as described previously (*23*). The amounts of the wild-type EF-Tu and the Q97P variant used were normalized in relation to their GDP binding activities.

Poly(U)-Directed Polymerization. The activities of wild-type and Q97P EF-Tu in poly(U)-directed polymerization were determined as previously described (*24*) with the indicated levels of the factors. *E. coli* EF-Ts in a 1:5 molar ratio to EF-Tu was present when indicated. The reaction mixtures were incubated for 10 min at 37 °C. The amount of [^{14}C]Phe incorporated into the polypeptide was determined as described (*24*). A blank representing the amount of label retained on the filter in the absence of EF-Tu (about 0.2 pmol) has been subtracted from each value. The amounts of the wild-type EF-Tu and the Q97P variant used were normalized in relation to their GDP binding activities.

RESULTS

Analysis of Structural Transitions in Domain 1 of EF-Tu. Domain 1 is formed by seven α-helices and six β-strands. Two conserved switch regions, switch I (residues 40−62) and switch II (residues 80−100), are central to conformational changes that occur in the transition from the GDP form to the GTP form of EF-Tu. In the EF-Tu·GDP complex switch I is formed by a short helix (A′, amino acids 46−50) and two short antiparallel β-strands (b′, residues 54−57; b″, residues 60−63) (Figures 1C and 2). In the EF-Tu·GDP form helix B in the switch II region encompasses residues 84−93. Major structural rearrangements occur in the transition to the EF-Tu·GTP complex (Figures 1D and 2). In the switch I region β-strand b′ is converted into a new helix (A″), and β-strand b″ becomes a coiled structure. In the switch II region helix B unwinds by one helical turn at the N-terminus and extends by 1 helical turn at the C-terminus and now comprises residues 87−97. This helix also tilts 42° relative to its position in EF-Tu·GDP. The changes in the molecular switch regions in domain 1 alter the surface of this domain in contact with domain 3.

EF-Tu is a highly conserved protein particularly in domain 1. Mammalian mitochondrial EF-Tu (EF-Tu$_{mt}$) is 55−60% identical to the prokaryotic factors. This high conservation is especially noted in critical regions such as switch I and switch II in domain 1 (Figure 2). However, there are some interesting exceptions to the high level of conservation generally observed. In the structural changes occurring in the conversion of EF-Tu from the GDP form to the GTP form, residue 97 (*E. coli* numbering) becomes the final residue in the shifted helix B in the switch II region. This residue is highly conserved as a Gln in prokaryotic EF-Tu (Figure 2). In contrast mammalian EF-Tu$_{mt}$ has a Pro in this position. Hence, it was of interest to examine the effect of a Pro at position 97 by the creation of an *E. coli* Q97P variant.

Expression of an E. coli Q97P Variant in E. coli. Site-directed mutagenesis was used to replace Gln97 with Pro in a His-tagged form of *E. coli* EF-Tu (*19*). The wild-type and Q97P variant of EF-Tu were expressed and purified as described in the Materials and Methods. The variant was expressed at levels comparable to those of the wild-type factor. Both the variant and wild-type factors were purified to 99% homogeneity as estimated by Coomassie Blue staining of an SDS−PAGE gel (data not shown).

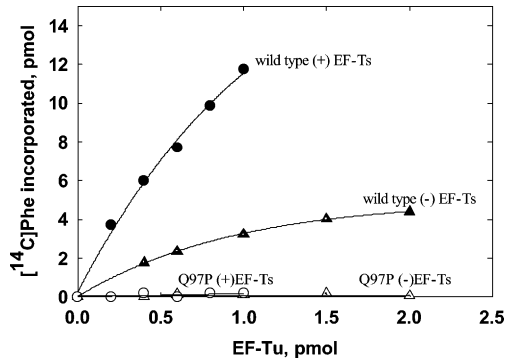

FIGURE 3: Poly(U)-directed polymerization of [^{14}C]Phe. The polymerization reactions were carried out as described in the Materials and Methods. Two independent preparations of wild-type and Q97P variant EF-Tu proteins purified separately were characterized. The displayed data are representative of trends observed in more than three experiments. EF-Ts was used as indicated. Key: ●, wild-type EF-Tu + EF-Ts; ▲, wild-type EF-Tu − EF-Ts; ○, Q97P variant + EF-Ts; △, Q97P variant − EF-Ts.

Activity of the E. coli EF-Tu Q97P Variant in Poly(U)-Directed Polymerization. The overall biological activity of EF-Tu Q97P was tested in the in vitro poly(U)-directed incorporation of [^{14}C]Phe into polypeptide. This assay measures all of the integral activities of EF-Tu including its ability to bind guanine nucleotides, to form a ternary complex with [^{14}C]Phe-tRNA^{Phe}, to deliver the ternary complex to the A-site of the ribosome, to hydrolyze GTP upon formation of the cognate codon−anticodon interaction, to release the [^{14}C]Phe-tRNA^{Phe} fully into the A-site, and to successfully dissociate from the ribosome. As indicated in Figure 3, the Q97P variant displayed no measurable activity in this assay either in the presence or in the absence of EF-Ts. These results clearly indicate that one or more of the individual steps which EF-Tu must carry out cannot occur in the Q97P variant. These steps were then examined systematically.

GDP Binding and Exchange. Preliminary measurements indicated that the Q97P variant retained its ability to bind GDP (data not shown). Hence, the equilibrium dissociation constant (K_d) for this complex was determined. The accurate determination of the K_d for the EF-Tu·GDP complex requires measurement of the concentration of GDP in the isolated EF-Tu preparations. Furthermore, it requires measurement of the percentage of EF-Tu in the preparation that is capable of binding GDP, allowing a calculation of the concentration of active EF-Tu present. Wild-type EF-Tu and the Q97P variant were isolated in the presence of 10 μM GDP to preserve their activities. Determination of the amount of GDP present in these preparations indicated that the actual concentration of GDP was equal to 10 μM plus a concentration of GDP equal to that of the EF-Tu present (data not shown). This concentration of GDP was too high to allow an accurate determination of the K_d for the EF-Tu·GDP complex. Chromatography of these preparations on Sephadex G-50 quantitatively removed all of the GDP present in excess over the concentration of active EF-Tu (data not shown). The concentration of GDP in such EF-Tu preparations was equal to that of the active EF-Tu protein. The concentration of active EF-Tu in each sample was determined immediately after chromatography using a saturating amount of [^{3}H]GDP and a filter binding assay as described in the Materials and Methods. This GDP concentration was used in all calculations of the K_d for a particular EF-Tu sample. The actual amount of EF-Tu active in binding GDP was determined in every experiment using this approach. As indicated in Table 1, the Q97P variant displayed slightly stronger GDP binding compared to the wild-type EF-Tu. This observation indicates that the Q97P substitution did not alter the GDP binding site in a significant manner.

Table 1: K_d GDP of Wild-Type and Q97P Variant EF-Tu[a]

	total [EF-Tu][b] (nM)	total [GDP][c] (nM)	[Tu·GDP] (nM)	K_d (nM)
wild type	6.9 ± 0.3	15 ± 0.74	3.4 ± 0.17	12 ± 1.6
	6.9 ± 0.3	28 ± 1.4	4.2 ± 0.21	15 ± 2.6
Q97P	6.9 ± 0.3	13 ± 0.64	3.8 ± 0.19	7.5 ± 1.2
	6.9 ± 0.3	27 ± 1.3	5.1 ± 0.25	7.7 ± 1.9

[a] Two independent preparations of wild-type and Q97P variant EF-Tu proteins purified separately were characterized. The error analysis was performed according to ref *25*. [b] It was observed that the amount of active molecules of EF-Tu decreases during storage. To properly assess the amount of active molecules in each experiment, a side-by-side reaction with saturating amounts of [^{3}H]GDP was carried out with the indicated amount of EF-Tu added. In these reactions 99.9% of the active EF-Tu molecules formed the [^{3}H]GDP·Tu complex. This measurement was used to precisely determine the concentration of EF-Tu for the calculation of the K_d in each experiment. [c] Total [GDP] included the [^{3}H]GDP added in the mix and the GDP added with the EF-Tu sample. The specific activity of the [^{3}H]GDP (cpm/pmol) was adjusted accordingly.

The slightly stronger interaction between the Q97P variant and GDP suggested either that k_{on} was faster or that the dissociation rate was slower, or both. The rate of GDP exchange with wild-type EF-Tu and with the Q97P variant was examined by incubating the respective EF-Tu·GDP complexes in the presence of [^{3}H]GDP for various times and measuring the amount of the labeled complex formed. As indicated in Figure 4A, the exchange of unlabeled GDP for external [^{3}H]GDP was slower for the Q97P variant than for the wild-type EF-Tu. The rate of formation of the labeled Q97P EF-Tu·[^{3}H]GDP complex was approximately 40% of that observed with the wild-type EF-Tu·[^{3}H]GDP complex at all time points. While the Q97P variant displayed a stronger GDP binding at equilibrium and slower rate of GDP exchange than the wild-type EF-Tu, the differences in GDP binding and exchange rate do not account for the Q97P variant's lack of activity in polymerization.

Under physiological conditions guanine nucleotide exchange is catalyzed by EF-Ts. As indicated in Figure 4B, EF-Ts stimulated the rate of nucleotide exchange about 5-fold with the wild-type EF-Tu and close to 10-fold with the Q97P variant (Figure 4). These results clearly indicate that the Q97P mutation does not significantly affect the nucleotide exchange reaction or the ability of EF-Ts to interact with EF-Tu.

GTP Binding. In the GTP-bound form of EF-Tu the effector loop of the switch I region transforms into helix A″ (53−59 aa) and reorients toward the GTP binding site away from domain 3 (Figures 1 and 2). In addition, helix B of the switch II region unwinds by one helical turn now encompassing residues 87−97 (Figure 1) and tilts 42° relative to its GDP position (Figure 1C,D). These structural changes enable residues from switches I and II to participate in binding the γ-phosphate of GTP. The Q97P substitution may alter the orientation of helix B in switch II and thus

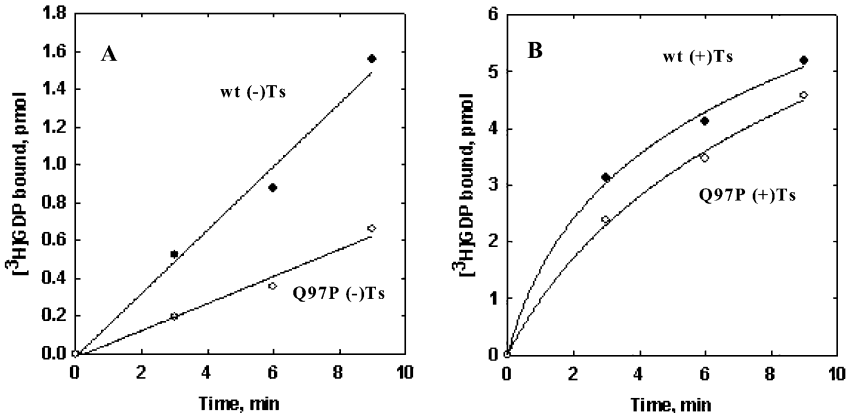

FIGURE 4: Time course of [^{3}H]GDP exchange with or without EF-Ts stimulation. The time courses of [^{3}H]GDP exchange into the EF-Tu·GDP complex were carried out as described in the Materials and Methods without EF-Ts (A) or with EF-Ts (B). Two independent preparations of wild-type and Q97P variant EF-Tu proteins purified separately were characterized. The displayed data are representative of trends observed in more than three experiments. Key: (A) ●, wild-type EF-Tu − EF-Ts; ○, Q97P variant − EF-Ts; (B) ●, wild-type EF-Tu + EF-Ts; ○, Q97P variant + EF-Ts.

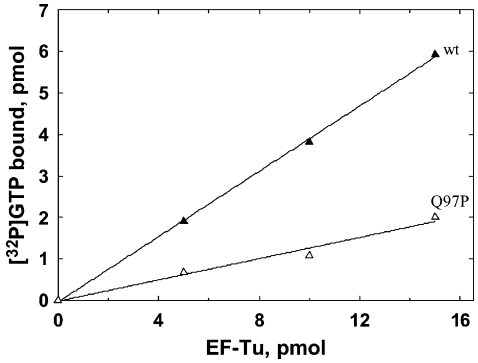

FIGURE 5: GTP binding activity of wild-type EF-Tu and the Q97P variant. The GTP binding activities of wild-type EF-Tu and its Q97P variant were tested as described in the Materials and Methods. Two independent preparations of wild-type and Q97P variant EF-Tu proteins purified separately were characterized. The displayed data are representative of trends observed in three independent experiments. Key: ▲, wild-type EF-Tu, △, Q97P variant EF-Tu. The amounts of EF-Tu indicated were based on the percentage of molecules active in GDP binding.

disrupt the contribution of residues in switch II to GTP binding. The exchange of GDP in the EF-Tu·GDP complex for GTP was examined as a measure of the ability of wild-type EF-Tu and the Q97P variant to bind GTP. For these experiments EF-Tu·GDP complexes were incubated with [γ-^{32}P]GTP in the presence of phosphoenol pyruvate and pyruvate kinase, and the amount of the EF-Tu·GTP complex formed was measured by a filter binding assay (Figure 5). The amounts of the wild-type EF-Tu and the Q97P variant used were normalized in relation to their GDP binding activities; i.e., equal amounts of each protein active in GDP binding were used. The reaction was carried out at subsaturating GTP levels since the K_d for EF-Tu·GTP is about 0.3 μM (*25*). The amount of GTP bound to the Q97P variant was about 1/3 of that bound to wild-type EF-Tu at equilibrium. However, this decrease in GTP binding activity cannot account for the complete loss of function in poly(U)-directed polymerization observed with the Q97P variant.

EF-Tu·GTP·Phe-tRNA^{Phe} Complex Formation. The structure of EF-Tu in the EF-Tu·GTP·Phe-tRNA^{Phe} complex is similar to the EF-Tu·GTP structure. Phe-tRNA^{Phe} makes use of the binding cleft formed in the EF-Tu·GTP complex and makes contacts with all three domains (Figure 6A). The CCA-Phe at the 3′-end of the tRNA binds in the cleft between domains 1 and 2, making extensive contacts with these domains. The 5′-end of the tRNA binds at the intersection of all three domains, making contact with a loop region from domain 2, contacting residues from helix A″ in switch I and helix B in switch II of domain 1 (Figure 6A). The side chain of Gln97 also participates in the formation of a network of hydrogen bonds among residues in domains 1 and 2 which form the amino acid binding pocket (Figure 6C).

An RNase A protection assay was used to explore the extent of ternary complex formation with the wild-type and Q97P variant of EF-Tu. This assay takes advantage of the observation that a significant portion of the aa-tRNA is protected from RNase cleavage when it is present in the ternary complex. The amounts of the wild-type and Q97P variant of EF-Tu used were normalized relative to their activities in binding GDP. As indicated in Figure 7, no detectable ternary complex was formed by the Q97P variant of EF-Tu. The inability of this mutated EF-Tu to form the ternary complex clearly explains its complete lack of activity in poly(U)-directed polymerization.

Due to the complexity of the aa-tRNA binding site involving contributions from all three domains of EF-Tu, the formation of the ternary complex tests the proper structure of EF-Tu in a more demanding manner than guanine nucleotide binding does; all three domains of EF-Tu must be in the proper orientation, thus creating the amino acid binding pocket and the cleft binding the acceptor stem/T-stem helix of the aa-tRNA. Therefore, ternary complex formation is a more sensitive gauge of any alteration in EF-Tu structure than either GDP or GTP binding.

DISCUSSION

From an alignment of prokaryotic and mammalian mitochondrial EF-Tu's, a nearly 100% conserved position, Gln97 in the prokaryotic factors, was identified as being replaced by Pro100 in the mammalian mitochondrial factors. In this study, it was demonstrated that an *E. coli* EF-Tu Q97P variant was active in guanine nucleotide binding but completely inactive in 3° complex formation.

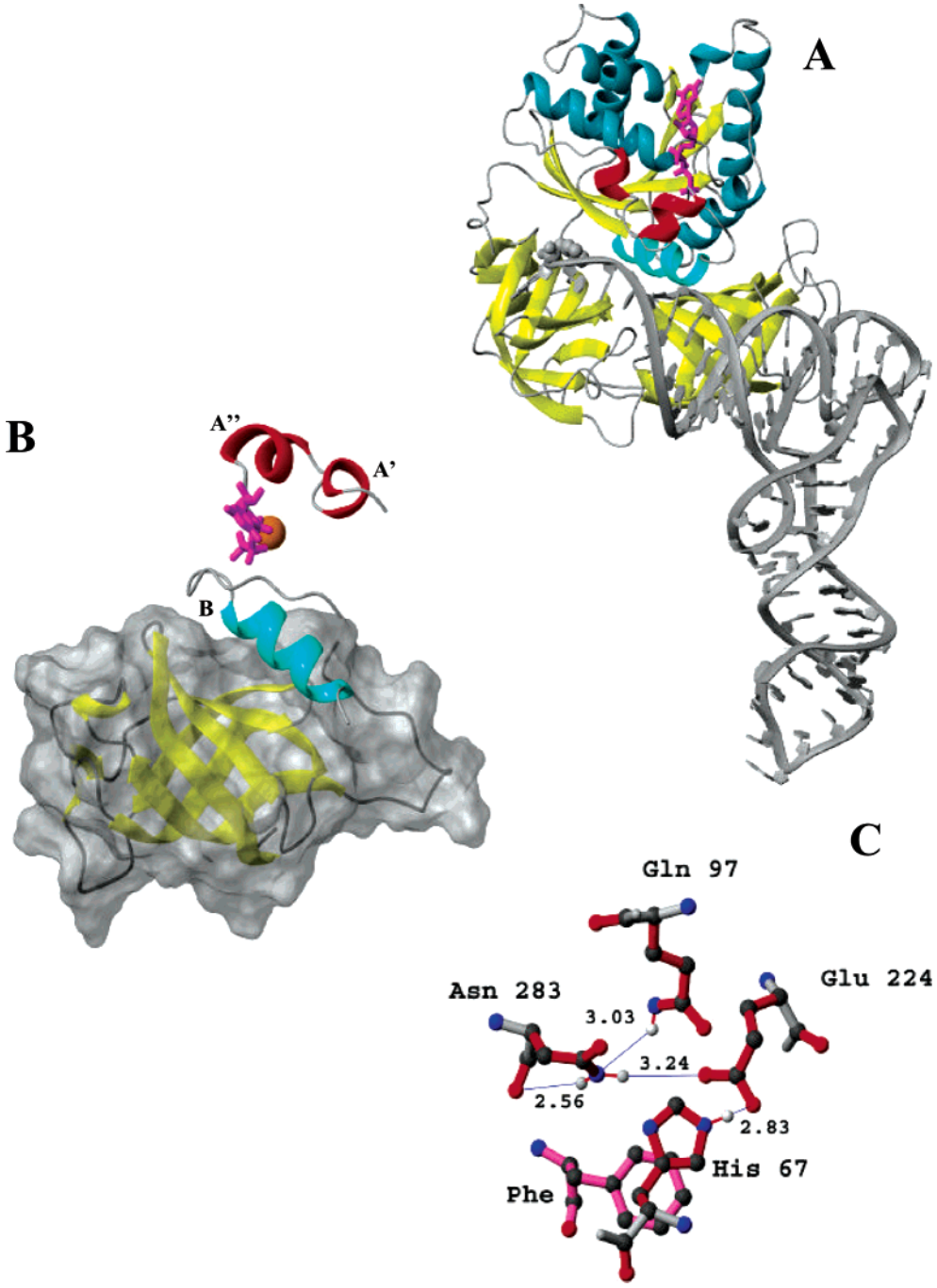

FIGURE 6: Interaction of domains 1−3 in the ternary complex of *T. aquaticus* EF-Tu. (A) The binding cleft for the aa-tRNA is formed between domains 1 and 3, while domains 1 and 2 form the amino acid binding pocket for the 3′-end CCA-Phe. β-Sheets are displayed in yellow, and α-helices are displayed in aquamarine with the exception of the switch I and II regions. Switch I is displayed in red, switch II in cyan, aa-tRNA in gray, the Phe attached to the tRNA space-filled in gray; and GTP in magenta. (B) Switch II helix B (cyan) of domain 1 traces tightly along the surface of domain 3 (gray). Switch I (red), GTP (magenta), and Mg^{2+} (orange) are displayed as well. (C) The side chain of Gln97 (Gln98 in the *T. aquaticus* numbering) participates in the formation of a H-bond network stabilizing the amino acid binding site. The backbone bonds are light gray, the side chain bonds are red, and the Phe attached to the tRNA is pink. Carbon atoms are shown in gray, nitrogen atoms in blue, oxygen atoms in red, and hydrogen atoms in white. Only hydrogen atoms participating in H-bonding in the pocket are displayed. The hydrogen bond length is displayed. The PDB number for (A)−(C) is 1TTT . The structures are displayed using MolMol (*28*) and Povray (http://www.povray.org).

The following model attempts to explain the biochemical data on the Q97P variant on a molecular basis using the structural information available. The substitution of Pro for Gln97 had little effect on the GDP binding site and probably does not affect the orientation of domain 1 in relation to domains 2 and 3 in the EF-Tu·GDP complex. A Swiss model of the EF-Tu·GDP complex was used to evaluate the potential accommodation of a Pro at position 97 and indicated that this change could be accommodated with no trouble (*26*, *27*). This idea is supported by the observation that the Q97P variant has a similar K_d for GDP binding. Further, the activity of the Q97P variant is stimulated normally by EF-Ts, which interacts with domains 1 and 3, and thus requires their proper orientation with respect to each other. In the EF-Tu·GDP structure Gln97 is located in the coil region following helix B (Figure 1A,C) and its side chain interactions are limited

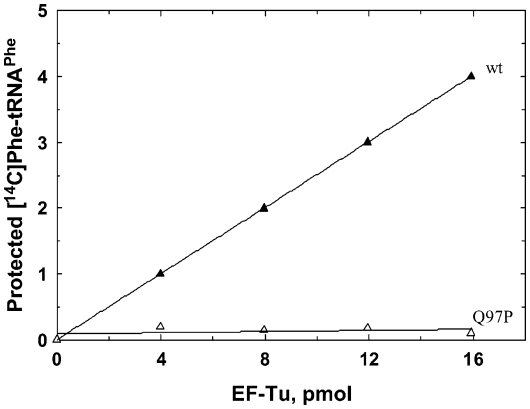

FIGURE 7: Formation of the EF-Tu·GTP·[^{14}C]Phe-tRNA^{Phe} complex. Ternary complex formation was determined using the protection from the nuclease digestion assay described in the Materials and Methods. No detectable ternary complex was formed with the Q97P variant. Key: ▲, wild-type EF-Tu; △, Q97P variant. The amounts of EF-Tu indicated were based on the percentage of molecules active in GDP binding. Two independent preparations of wild-type and Q97P variant EF-Tu proteins purified separately were characterized. The displayed data are representative of trends observed in more than three independent experiments.

to neighboring amino acids. Thus, the Q97P change may be accommodated without causing a structural disturbance that would result in a significant decrease in GDP binding and EF-Ts stimulation.

The role of Gln97 in the wild-type EF-Tu·GTP complex differs significantly from its role in the EF-Tu·GDP complex. Due to the extension of helix B in the GTP complex, Gln97 is positioned at the C-terminus of helix B in the switch II region (Figure 1B,D). The Q97P mutation might, thus, be expected to alter the GTP binding site in the EF-Tu·GTP complex by affecting the orientation of helix B. An altered orientation could weaken the interaction of Gly83 preceding helix B with the γ-phosphate of GTP. This idea is supported by the 3-fold lower activity of the Q97P variant in GTP binding compared to that of wild-type EF-Tu.

Position 97 is also potentially important for the binding of aa-tRNA to EF-Tu. GTP binding results in the rotation of helix B relative to the rest of domain 1 with the concomitant rotation of domain 1 with respect to domains 2 and 3. As a result of this conformational change, the side chain of Gln97 now contributes to the hydrogen bond network stabilizing the amino acid binding pocket (Figure 6C). The Q97P mutation completely eliminates ternary complex formation. This observation indicates that the aa-tRNA binding site is not being created properly in the variant. Two possible scenarios can be suggested to explain this effect: (i) improper orientation of helix B in the switch II region prevents the creation of the proper aa-tRNA binding cleft or (ii) the loss of interaction of the Gln97 side chain with residues in domain 2 lining the amino acid binding pocket causes a constriction of the amino acid binding pocket. Each of these scenarios is discussed in more detail below.

The creation of the proper aa-tRNA binding site upon GTP binding to EF-Tu is triggered by creation of helix A″ of switch I and the rotation of helix B in switch II. These structural changes cause domain 1 to rotate in relation to the rigid body of domains 2 and 3 by 90°, creating the binding cleft for the Phe-tRNA^{Phe} (Figure 6). Gln97 is positioned at the C-terminus of helix B in the GTP form of EF-Tu. Helix B lies along the surface of domain 3 in EF-Tu·GTP (Figure 6B). The presence of a Pro at the C-terminus of helix B may change the orientation of this helix in the GTP form of EF-Tu, disrupting the proper binding surface between domains 1 and 3 and causing an imperfect interaction between these two domains. Such an altered orientation would certainly disrupt the binding cleft for the aa-tRNA. Furthermore, residues G1, C2, and G3 in Phe-tRNA^{Phe} contact N-terminal residues of helix B including Arg86, Tyr87, Lys89, and Asn90. An improper orientation of helix B could prevent these interactions from occurring correctly. To explore possible structural consequences of the Q97P mutation, a Swiss model was used to place a proline residue at position 97 of EF-Tu in the ternary complex. Since position 97 is a kinked backbone of helix B in the GTP conformation, the proline side chain can be sterically accommodated without interfering with other helical residues. The Φ and Ψ angles of Gln97 in the ternary complex are $-112.5°$ and $-4.85°$. These angles are within the angles accommodated by Pro, but they are not commonly observed. Although Pro97 is not structurally prohibited from occupying these Φ and Ψ angles, forcing the Pro residue into these angles may be thermodynamically unfavorable.

Under the second scenario, the amino acid binding pocket may constrict due to the loss of the hydrogen bonding from the Gln97 side chain to the residues lining the amino acid binding pocket. Gln97 hydrogen bonds to Asn283 (Figure 6C). Asn283 hydrogen bonds to Glu224, which, in turn, forms a hydrogen bond with His67. His67 stacks on the top of the phenyl ring of CCA-Phe. Without the stabilization of the binding pocket by the side chain interaction with Gln97, the binding pocket may constrict, preventing the binding of the CCA-aa end of the tRNA. This event would account for the Q97P variant's lack of Phe-tRNA^{Phe} binding.

A combination of the two scenarios described is possible. The side chain of Gln97 may stabilize the amino acid binding pocket and further secure proper orientation of helix B. The Q97P substitution may weaken or partially close the amino acid binding pocket while disorienting helix B at the same time. In this manner the aa-tRNA binding cleft would not be created due to the improper surface of domain 1 facing domain 3, and the amino acid binding pocket may not be able to accept the bulky Phe side chain due to its constriction.

Clearly the data provided here indicate that *E. coli* EF-Tu cannot accommodate a Pro residue at position 97. One must then wonder why Pro is conserved in this position in mammalian EF-Tu$_{mt}$. One reasonable hypothesis is that, in the GTP-complex and in the ternary complex formed by mammalian EF-Tu$_{mt}$, helix B does not extend as far as it does in the prokaryotic factors and does not include the Pro at the position equivalent to Gln97. In this case this residue may not be central to the formation of the interface between domains 1 and 3 that is necessary for the formation of the bacterial ternary complex. In support of this idea is the observation that contacts between domains 1 and 3 in the EF-Tu$_{mt}$·GDP complex are different from those observed in the corresponding bacterial complex. Indeed, domain 1 is positioned at a somewhat different angle relative to domain 3 in the bacterial complexes compared to the EF-Tu$_{mt}$·GDP complex. It is reasonable to suppose that residue 97 is, then, not central to the interdomain contacts required for the

formation of the ternary complex with the mammalian EF-Tu_{mt}. A second reasonable hypothesis for the accommodation of Pro in EF-Tu_{mt} is that the construction of the amino acid binding pocket does not require a hydrogen bond contribution from the side chain of the residue in position 97 in the mitochondrial factor.

The Q97P variant of *E. coli* EF-Tu demonstrates the precarious synergy between the domains of EF-Tu which is necessary to create a functional binding site for the aa-tRNA. In this case an alteration of one amino acid may prevent this synergy by disrupting an important hydrogen bond between domains 1 and 2 and by preventing proper surface formation between domains 1 and 3. The Q97P variant of EF-Tu thus exemplifies the precise relationship between the structure and function of a protein.

ACKNOWLEDGMENT

We thank Dr. Dorothy Erie (Department of Chemistry, University of North Carolina) for helpful discussions on the design of several of the experiments.

REFERENCES

1. Krab, I., and Parmeggiani, A. (1998) EF-Tu, a GTPase odyssey, *Biochim. Biophys. Acta 1443*, 1−22.
2. Abel, K., Yoder, M. D., Hilgenfeld, R., and Jurnak, F. (1996) An alpha to beta conformational switch in EF-Tu, *Structure 4*, 1153−1159.
3. Jurnak, F. (1985) Structure of the GDP domain of EF-Tu and location of the amino acids homologous to ras oncogene proteins, *Science 230*, 32−36.
4. Song, H., Parsons, M. R., Rowsell, S., Leonard, G., and Phillips, S. E. (1999) Crystal structure of intact elongation factor EF-Tu from *Escherichia coli* in GDP conformation at 2.05 Å resolution, *J. Mol. Biol. 285*, 1245−1256.
5. Polekhina, G., Thirup, S., Kjeldgaard, M., Nissen, P., Lippmann, C., and Nyborg, J. (1996) Helix unwinding in the effector region of elongation factor EF-Tu-GDP, *Structure 4*, 1141−1151.
6. Andersen, G., Thirup, S., Spremulli, L. L., and Nyborg, J. (2000) High-resolution crystal structure of bovine mitochondrial EF-Tu in complex with GDP, *J. Mol. Biol. 297*, 421−436.
7. Berchtold, H., Reshetnikova, L., Reiser, C., Schirmer, N., Sprinzl, M., and Hilgenfeld, R. (1993) Crystal structure of active elongation factor Tu reveals major domain rearrangements, *Nature 365*, 126−132.
8. Kjeldgaard, M., Nissen, P., Thirup, S., and Nyborg, J. (1993) The crystal structure of elongation factor EF-Tu from *Thermus aquaticus* in the GTP conformation, *Structure 1*, 35−50.
9. Kawashima, T., Berthet-Colominas, C., Wulff, M., Cusack, S., and Leberman, R. (1996) The structure of the *Escherichia coli* EF-Tu:EF-Ts complex at 2.5 Å resolution, *Nature 379*, 511−518.
10. Wang, Y., Jiang, Y., Meyering-Voss, M., Sprinzl, M., and Sigler, P. (1997) Crystal structure of the EF-Tu-EF-Ts complex from *Thermus thermophilus*, *Nat. Struct. Biol. 4*, 650−656.
11. Nissen, P., Kjeldgaard, M., Thirup, S., Polekhina, G., Reshetnikova, L., Clark, B., and Nyborg, J. (1995) Crystal structure of the ternary complex of Phe-$tRNA^{Phe}$, EF-Tu and a GTP analog, *Science 270*, 1464−1472.
12. Nissen, P., Thirup, S., Kjeldgaard, M., and Nyborg, J. (1999) The crystal structure of Cys-$tRNA^{Cys}$-EF-Tu-GDPNP reveals general and specific features in the ternary complex and in tRNA, *Structure 7*, 143−156.
13. Burkhardt, N., Junemann, R., Spahn, C. M., and Nierhaus, K. H. (1998) Ribosomal tRNA binding sites: three-site models of translation, *Crit. Rev. Biochem. Mol. Biol. 33*, 95−149.
14. Suttle, D. P., Haralson, M. A., and Ravel, J. M. (1973) Initiation factor 3 requirement for the formation of initiation complexes with synthetic oligonucleotides, *Biochem. Biophys. Res. Commun. 51*, 376−382.
15. Eberly, S. L., Locklear, V., and Spremulli, L. L. (1985) Bovine mitochondrial ribosomes. Elongation factor specificity, *J. Biol. Chem. 260*, 8721−8725.
16. Zhang, Y., Sun, V., and Spremulli, L. L. (1997) Role of domains in *Escherichia coli* and mammalian mitochondrial elongation factor Ts in the interaction with elongation factor Tu, *J. Biol. Chem. 272*, 21956−21963.
17. Ravel, J. M., Shorey, R. L., Froehner, S., and Shive, W. (1968) A study of the enzymic transfer of aminoacyl-RNA to *Escherichia coli* ribosomes, *Arch. Biochem. Biophys. 125*, 514−526.
18. Ito, W., Ishiguro, H., and Kurosawa, Y. (1991) A general method for introducing a series of mutations into cloned DNA using the polymerase chain reaction, *Gene 102*, 67−70.
19. Zhang, Y., Li, X., and Spremulli, L. L. (1996) Role of the conserved aspartate and phenylalanine residues in prokaryotic and mitochondrial elongation factor Ts in guanine nucleotide exchange, *FEBS Lett. 391*, 330−332.
20. Sambrook, J., Fritsch, E., and Maniatis, T. (1989) *Molecular Cloning: A Laboratory Manual*, Cold Spring Harbor Laboratory Press, Cold Spring Harbor, NY.
21. Woriax, V., Burkhart, W., and Spremulli, L. L. (1995) Cloning, sequence analysis and expression of mammalian mitochondrial protein synthesis elongation factor Tu, *Biochim. Biophys. Acta 1264*, 347−356.
22. Cai, Y.-C., Bullard, J. M., Thompson, N. L., and Spremulli, L. L. (2000) Interaction of mitochondrial Elongation Factor Tu with aminoacyl-tRNA and Elongation Factor Ts, *J. Biol. Chem. 275*, 20308−20314.
23. Louie, A., Ribeiro, S., Reid, B., and Jurnak, F. (1984) Relative affinities of all *Escherichia coli* aminoacyl-tRNAs for elongation factor Tu-GTP, *J. Biol. Chem. 259*, 5010−5016.
24. Schwartzbach, C., and Spremulli, L. L. (1991) Interaction of animal mitochondrial EF-Tu:EF-Ts with aminoacyl-tRNA, guanine nucleotides and ribosomes, *J. Biol. Chem. 266*, 16324−16330.
25. Miller, D., and Weissbach, H. (1970) Studies on the purification and properties of factor Tu from *E. coli*, *Arch. Biochem. Biophys. 141*, 26−37.
26. Guex, N., and Peitsch, M. C. (1997) SWISS-MODEL and the Swiss-PdbViewer: an environment for comparative protein modeling, *Electrophoresis 18*, 2714−2723.
27. Peitsch, M., Wells, T., Stampf, D., and Sussman, J. (1995) The Swiss-3D image collection and PDB-browser on the world wide web, *Trends Biochem. Sci. 20*, 82−85.
28. Koradi, R., Billeter, M., Wüthrich, K. (1996) MOLMOL: a program for display and analysis of macromolecular structures, *J. Mol. Graphics 14*, 51−55.

BI034855A